GRID-ASSOCIATED WIND AND SOLAR COGENERATION WITH VOLTAGE SOURCE BACK-TO-BACK CONVERTERS

RUDROJUSHIVAKUMAR[1]KOMPELLI SAIKUMAR[2] KAMTAM YASHWANTH[3]

MYADARAVENI PRAVALIKA[4] SANDELA VIPIN[5]

[1]Assistant Professor, Department of EEE, Jyothishmathi institute of technology and science,Nustulapur, Karimnagar, TS, India

[2,3,4,5]UG students, Department of EEE, Jyothishmathi institute of technology and science, Nustulapur, Karimnagar, TS, India

Abstract: This project introduces a new topology, yet simple and efficient, for a grid-connected wind-solar cogeneration system. A permanent magnet synchronous generator-based full-scale wind turbine is interconnected to the utility-grid via back-to-back voltage-source converters (VSCs). The dc-link capacitor has been utilized to directly interface a photovoltaic solar generator. No dc/dc conversion stages are required, and hence, the hybrid system is simple and efficient. Moreover, the proposed topology features an independent maximum power point tracking for both the wind and the solar generators to maximize the extraction of the renewable energy. The regulation of the VSCs is achieved via the vector control in the rotating reference frame. The detailed small-signal models for the system components are developed to characterize the overall stability. The influence of the utility-grid faults on the performance of the proposed system is also investigated. Nonlinear time-domain simulation results under different operating conditions are presented to validate the effectiveness of the proposed topology.

Keywords:solar power generation, wind power generation, AC-DC power converters, DC-AC power converters, maximum power point tracking

I.INTRODUCTION

The cost of the wind and solar generation has been rapidly falling since the last decade. Driven by their economic and technical incentives, the global installed solar and wind power capacity has approached 303 Gigawatt (GW) and 487 GW in 2016, as compared to 6 GW and 74 GW in 2006, respectively [1]. Due to the intermittent and unregulated nature of the wind and solar energy, power-electronic converters are utilized as an interfacing stage to the load-side or the utility-grid to create distributed generation units [2], [3]. In the literature, most of the distributed generation systems are solely dedicated for one form of renewable resources, e.g., a solar energy as in [4], [5] or a wind energy as presented in [6]– [8]. In order to maximize the benefits of the available renewable resources, the combination of the wind and solar generators in one location has been recently considered [9]. The hybrid wind and solar energy cogeneration features the following characteristics; 1) the availability of the wind and solar energy is generally complementary, and hence combining both forms of energy increase the overall operational efficiency. 2) the hybrid wind and solar co-generators optimize the utilization of lands resources due to the reduced footprint of the combined system, and hence improves the capital investments. 3) as compared to the static solar generators, the combined wind and solar cogeneration systems are more dynamically capable to support the utility-grid thanks to the available moment of inertia in the mechanical parts of the wind generators [8]. 4) having two sources of energy increases the generation reliability [9], [10]. In the literature, the grid-connected wind and solar cogenerators are not widely addressed [9]– [15]. On the contrary, several wind and solar hybrid systems are available for the standalone off-grid applications [10], [16]. An optimal sizing method for a wind-solar-battery system in the grid-connected and standalone applications has been proposed in [10]. A systematic stochastic planning for a hybrid system consisting of the wind and solar systems is proposed in [11]. In [12]– [14], the integration of the renewable energy resources has been improved by utilizing multiple-input converters. A buck/buck-boost fused dc-dc converter is proposed in [12]. A dc-dc converter

with a current-source interface, and a coupled transformer are proposed in [13] and [14], respectively. Beside the relatively complex structured topologies in [12]– [14], the proposed systems are based on the dc power distribution which might not be the ideal distribution medium in the ac-dominated power systems. Moreover, the introduced systems are proposed for relatively low-power levels and have not been tested in high-power applications. A standalone hybrid wind and solar system is proposed in [16], [17] including a diesel engine generator and a storage battery. On the small-scale level, a single-phase hybrid system has been proposed in [18] whereas a laboratory-scale system is introduced in [19], [20]. Generally, the system structure in [16]– [20] comprises a common dc-bus that interfaces several parallel connected converters-interfaced renewable energy resources, which might reduce the overall system efficiency and increase the cost [12]. Moreover, the cascaded connection of power converters requires rigorous controllers design and coordination to avoid the induced interactions dynamics among the tightly regulated power converters, which might yield instabilities. A back-to-back (BtB) voltage-source converter (VSC) connected to a doubly-fed induction generator is used to interface a dc-dc converter-interfaced photovoltaic (PV) generator and an energy storage unit in [19]. In [20], a PV generator charging a battery bank and interfaced to a wind driven induction generator via a VSC is proposed. The hybrid wind-solar systems in [19], [20] highlights the efficient integration of the renewable energy resources with the minimal utilization of power electronic conversion stages. However, these systems are proposed for specific off-grid applications. Up to the authors' best knowledge, the combination of the grid-connected wind-solar systems has been mainly addressed in [15]. The system in [15] comprises a BtB VSCs to interface the solar and wind generators to the utility-grid. On the machine-side-VSC, the dc-link voltage is regulated to the maximum power-point tracking (MPPT) value of the PV panel by an outer loop Proportional-and-Integral (PI) dc voltage controller. The reference values of the machine-side currents are calculated using the synchronous detection method, and a hysteresis current controller is utilized for the regulation. On the grid-sideVSC, a hysteresis grid-current controller is used to inject the total currents to the utility-grid. In spite of the potential benefits of the proposed system in [15], the following challenges are noted; 1) the MPPT of either the PV and wind power involves the operation of both VSCs, which in some cases might decrease the system reliability and increase the losses. For instance, if the wind velocity is lower than the cut-off speed of the wind turbine, i.e., no wind power, the machine-side VSC may be unable to track the solar PV MPPT dc-link voltage [15]. 2) the dc-link voltage is regulated from the machine-side, and there is no a direct regulation on the speed of the wind turbine, i.e., a servo operation. 3) the machine and grid-side currents are controlled using hysteresis controllers resulting in a variable switching frequency and higher harmonic contents. Motivated by the promising benefits of the hybrid wind-solar generation systems, and the challenges facing the proposed system in [15], this paper introduces a new topology, yet simple and efficient to interface both the wind and solar generators into the utility-grid. The contributions of this paper are as follows: 1) The realization of the combined grid-connected wind and solar generators using BtB VSCs with no extra power electronic switches. 2) Unlike the proposed system in [15], the voltage-source rectifier (VSR) is solely responsible for MPPT of the wind generator whereas the voltage-source inverter (VSI) harvests the maximum PV power by regulating the dc-link voltage to inject the total dc power into the utility-grid. 3) The development of the entire small-signal state-space model of the proposed system to characterize the overall system stability. 4) The performance of proposed hybrid system has been investigated under different operating conditions including the utility-grid faults using time-domain simulations.

II.LITERATURE SURVEY

[1] Renewable Energy Policy Network for the 21st Century, "Advancing the global renewable energy transition," REN21 Secretariat, Paris, France, 2017.

The global electrical energy consumption is rising and there is a steady increase of the demand on the power capacity, efficient production, distribution and utilization of energy. The traditional power systems are changing globally, a large number of dispersed generation (DG) units, including both renewable and non-renewable energy sources such as wind turbines, photovoltaic (PV) generators, fuel cells, small hydro, wave generators, and gas/steam

powered combined heat and power stations, are being integrated into power systems at the distribution level. Power electronics, the technology of efficiently processing electric power, play an essential part in the integration of the dispersed generation units for good efficiency and high performance of the power systems. This paper reviews the applications of power electronics in the integration of DG units, in particular, wind power, fuel cells and PV generators.

[2] F. Blaabjerg, Z. Chen, and S. B. Kjaer, "Power electronics as efficient interface in dispersed power generation systems," IEEE Trans. Power Electron., vol. 19, no. 5, pp. 1184–1194, Sep. 2004.

The use of distributed energy resources is increasingly being pursued as a supplement and an alternative to large conventional central power stations. The specification of a power-electronic interface is subject to requirements related not only to the renewable energy source itself but also to its effects on the power-system operation, especially where the intermittent energy source constitutes a significant part of the total system capacity. In this paper, new trends in power electronics for the integration of wind and photovoltaic (PV) power generators are presented. A review of the appropriate storage-system technology used for the integration of intermittent renewable energy sources is also introduced. Discussions about common and future trends in renewable energy systems based on reliability and maturity of each technology are presented

[3] J. Carrasco et al., "Power-electronic systems for the grid integration of renewable energy sources—a survey," IEEE Trans. Ind. Electron., vol. 53, no. 4, pp. 1002–1016, Jan. 2006.

This paper proposes a control strategy for a single-stage, three-phase, photovoltaic (PV) system that is connected to a distribution network. The control is based on an inner current-control loop and an outer DC-link voltage regulator. The current-control mechanism decouples the PV system dynamics from those of the network and the loads. The DC-link voltage-control scheme enables control and maximization of the real power output. Proper feedforward actions are proposed for the current-control loop to make its dynamics independent of those of the rest of the system. Further, a feedforward compensation mechanism is proposed for the DC-link voltage-control loop, to make the PV system dynamics immune to the PV array nonlinear characteristic. This, in turn, permits the design and optimization of the PV system controllers for a wide range of operating conditions. A modal/sensitivity analysis is also conducted on a linearized model of the overall system, to characterize dynamic properties of the system, to evaluate robustness of the controllers, and to identify the nature of interactions between the PV system and the network/loads. The results of the modal analysis confirm that under the proposed control strategy, dynamics of the PV system are decoupled from those of the distribution network and, therefore, the PV system does not destabilize the distribution network. It is also shown that the PV system dynamics are not influenced by those of the network (i.e., the PV system maintains its stability and dynamic properties despite major variations in the line length, line X / R ratio, load type, and load distance from the PV system).

[4] A. Yazdani and P. P. Dash, "A control methodology and characterization of dynamics for a photovoltaic (PV) system interfaced with a distribution network," IEEE Trans. Power Del., vol. 24, no. 3, pp. 1538–1551, Jul. 2009.

A photovoltaic (PV) generator is internally a power limited non-linear current source having both constant current and voltage like properties depending on the operating point. This paper investigates the dynamic properties of a PV generator and demonstrates that it has a profound effect on the operation of the interfacing converter. The most important properties an input source should have in order to emulate a real PV generator are defined. These properties are important, since a power electronic substitute is often used in the validation process instead of a real PV generator. This paper also qualifies one commercial solar array simulator as an example in terms of the defined properties. Investigations are based on extensive practical measurements from dc-dc as well as three- and single-phase dc-ac converters.

[5] L. Nousiainen et al., "Photovoltaic generator as an input source for power electronic converters," IEEE Trans. Power Electron., vol. 28, no. 6, pp. 3028–3038, Jun. 2013.

A photovoltaic (PV) generator is internally a power limited non-linear current source having both constant current and voltage like properties depending on the operating point. This paper investigates the dynamic properties of a PV generator and demonstrates that it has a profound effect on the operation of the interfacing converter. The most important properties an input source should have in order to emulate a real PV generator are defined. These properties are important, since a power electronic substitute is often used in the validation process instead of a real PV generator. This paper also qualifies one commercial solar array simulator as an example in terms of the defined properties. Investigations are based on extensive practical measurements from dc-dc as well as three- and single-phase dc-ac converters.

[6] N. Strachan and D. Jovcic, "Stability of a variable-speed permanent magnet wind generator with weak ac grids," IEEE Trans. Power Del., vol. 25, no. 4, pp. 2279–2788, Oct. 2010.

The operation of high-power wind generators with weakened ac grids has historically been difficult because of stability and power quality issues. This paper presents an analytical stability study of a variable-speed directly-driven permanently-excited 2-MW wind generator connected to ac grids of widely varying strength and very weak grids. The generator includes two back-to-back full-scale vector controlled 3-level neutral-point-clamped (NPC) voltage-source-converters (VSC). A 47th order small-signal analytical wind generator model is developed within MATLAB, and a summary of the model structure and controls is given. Model verification is demonstrated for fast and slow system variables employing detailed simulation software PSCAD/EMTDC. An eigenvalue stability study for weak ac networks is presented, and qualitative conclusions about inherent system dynamics and stability characteristics are given. These insights are employed to study the design of an ac voltage controller for weak ac networks. Two alternative controller designs are studied for their potential to enhance system robustness to changes in ac grid strength.

III.PROPOSED HYBRID WIND-SOLAR GENERATOR

As shown in Fig. 1, the proposed system consists of a VSR to interface the wind generator, and a VSI to connect the hybrid cogeneration system into the utility-grid. The PV generator is directly connected to the dc-link capacitor of the BtB VSCs via a dc cable. The VSR and VSI are two-level converters consisting of six cells; each comprises an insulated-gate-bipolartransistor (IGBT) in parallel with a diode. In the following subsections, the complete modelling and control of the proposed system are provided.

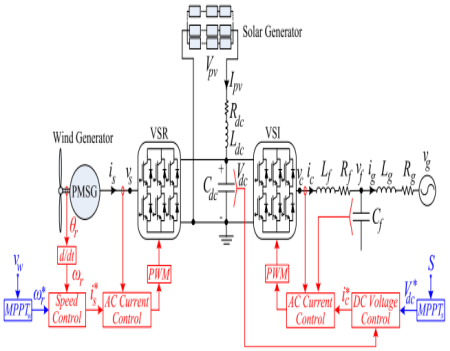

Fig. 1. Proposed wind-solar cogeneration system.

a) Wind Generator

A full-scale wind turbine (FSWT) utilizing a permanent magnet synchronous generator (PMSG) is selected for its low maintenance and low operational cost [2]. The wind turbine model is represented as follows

$$P_m = \frac{1}{2} C_p(\beta, \lambda)\, \rho \pi R^2 v_{wind}^3, \; \lambda = \frac{R\omega_r}{v_{wind}} \quad (1)$$

where Pm is the mechanical power captured by the wind turbine bladed; Cp is the rotor power coefficient which is a nonlinear function of the blade pitch angle β and the tip-speed ratio λ; ρ is the air density; R is the radius of the wind turbine blade; and vwind is the wind speed. In this paper, β is set to zero in the normal operating conditions to maximize the wind power generation [13]. The PMSG is modelled as following,

$$\bar{v}_s = R_s \bar{i}_s + L_s \frac{d\bar{i}_s}{dt} + j\mathcal{P}\omega_r (\psi + L_s \bar{i}_s) \quad (2)$$

$$J\frac{d}{dt}\omega_r + \beta\omega_r = \frac{3}{2}\mathcal{P}\psi I_{sq} - T_m \quad (3)$$

where v¯s and ¯is are the stator voltage and current in the complex vectors representation, respectively, where a complex vector x¯ = Xd + jXq such that Xd and Xq are the direct (d−) and quadrature (q−) components of x¯ in the rotating reference frame; Rs and Ls are the stator-winding resistance and inductance, respectively; j is the imaginary unit number; ψ is the flux linkage of the rotor magnets; ωr is the mechanical speed of the rotor; P is the number of poles pairs; Tm is the mechanical torque; whereas J and β are the motor inertia, and viscous friction, respectively.

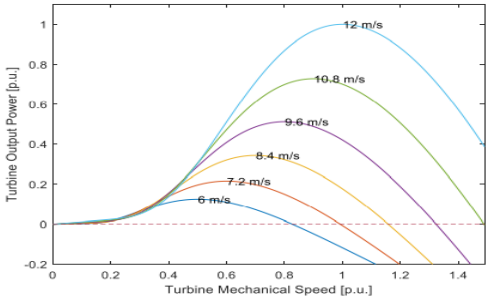

Fig. 2. Mechanical characteristics of the wind turbine at different wind speeds.

Fig.2 shows the relationship between the mechanical rotor speed and the generated turbine power at different wind speeds. The maximum wind power can be generated if the rotor speed is optimally regulated to follow the wind speed variations. As shown in Fig. 1, this role can be achieved at the VSR-side using the MPPT for the wind generator (MPPTw) that utilizes the wind speed (vw) to generate the reference value of PMSG rotor speed (ω∗ r) [17], [19]

b) Machine-Side Voltage Source Rectifier (VSR)

The VSR is utilized to capture the maximum wind power by regulating the mechanical rotor speed of the PMSG to follow the MPPTw characteristics in Fig. 2, using the PI speed controller (Gs(s)) in (4).

$$I_{sq}^{*} = (\omega_r^{*} - \omega_r)\, G_s(s),\ I_{sd}^{*} = 0 \quad (4)$$

The PI speed controller (Gs (s) = gps + gis/s) is implemented in the outer loop, where s represents the differential operator and the superscript "∗" denotes the reference values of the variable. The speed controller regulates the PMSG speed to the optimal value (ω∗r) and dictates the q- component of stator current reference (I∗sq), whereas I∗sd is set to zero to operate at maximum produced torque [19]. Solving (3) and (4), assuming Isq ≈ I∗sq within the bandwidth of the speed controller, and setting gis/gps = β/J, the closed loop transfer function of the speed controller (Gs(s)) becomes ωr /ω∗ r = (3 2 Pψgp s J)/(s + 3 2 Pψgp s J), where the bandwidth of the speed controller is 3 2Pψgps/J [rad/s], and is selected around 0.1 of the bandwidth of the inner PI current controller (Gi(s)) [shown in (5)]. The speed controller parameters, i.e., gps and gis , can be tuned accordingly. The PI current controller (Gi(s) = gpi + gii/s) is implemented in the inner loop, so that the generated stator currents of the PMSG follow the corresponding references in (5).

$$\bar{v}_s = \left(\bar{i}_s^{*} - \bar{i}_s\right) G_i(s) + j\mathcal{P}\omega_r^{\circ} L_s \bar{i}_s + j\mathcal{P}\psi H\omega_r \quad (5)$$

Note that jPω◦ rLs ¯is are the decoupling loops; whereas the superscript "◦" denotes the steady-state value of the variable.

Similar to the speed controller design, the current controller is designed by solving (2) and (5). By setting gii/gpi = Rs/Ls , the closed loop transfer function of the current controller becomes; Isd /I∗sd = 1/(τis + 1), where the bandwidth of the current controller is 1/τi = gpi/Ls [rad/s], and is selected around 0.1-0.2 of the switching frequency.

c)Grid-Side Voltage Source Inverter (VSI)

As shown in Fig.1, the ac-side of the VSI is terminated by an inductive filter (Lf) with an internal resistance (Rf) and a shunt capacitor (Cf). The rms value of the three-phase terminal voltage and currents of the VSI are vc and ic, respectively. The utility-grid-impedance comprises an inductive part (Lg) in series with the equivalent resistance of the line (Rg); vg and ig are the utility-grid three-phase rms voltage and currents, respectively. The Lf − Cf filter and the utility-grid impedance are modelled as following;

$$\bar{v}_c = \bar{v}_f + R_f\bar{i}_c + L_f\frac{d\bar{i}_c}{dt} + j\omega L_f\bar{i}_c \quad (6)$$

$$\bar{v}_f = \bar{v}_g + R_g\bar{i}_g + L_g\frac{d\bar{i}_g}{dt} + j\omega L_g\bar{i}_g \quad \textbf{(7)}$$

$$\bar{i}_c = C_f\frac{d\bar{v}_f}{dt} + \bar{i}_g + j\omega C_f\bar{v}_f \quad \textbf{(8)}$$

Using (5.9), the VSI is regulated by the vector control topology where a phase-locked-loop (PLL) is used to synchronize the converter to the utility-grid.

$$\omega = \omega^{\circ} + \frac{V_{fg}^{c}}{V_{fd}^{c}}K_{\delta}(s) \quad (9)$$

In (10), (Kδ (s) = Kpδ + Kiδ /s) is a PI controller implemented in the PLL structure to set the q-component of the PCC voltage (Vcq) to zero and generate the synchronization angle δ(t), where δ(t) = ∫ ω(t)dt, and the superscript "c" denotes the converter reference frame. Under transient conditions, the angle δ(t) oscillates to resynchronize the converter with the utilitygrid and eventually becomes zero in the steady-state conditions. The main advantage of the vector control is the decoupling between the active and reactive power regulation. As Vcq is set to zero by (10) and assuming Vcd is constant, the active power injection from the VSI(Pvsi) can be regulated by controlling Icd whereas the reactive power (Qvsi) is solely dependent on Icq, as shown in (5.10).

$$P_{vsi} = Real\left\{1.5\bar{v}_c\bar{i}_c^{conjugate}\right\} = 1.5V_{cd}I_{cd},$$

$$Q_{vsi} = Iamginary\left\{1.5\bar{v}_c\bar{i}_c^{conjugate}\right\} = -1.5V_{cd}I_{cq}. \quad \textbf{(10)}$$

IV.SIMULATION RESULTS

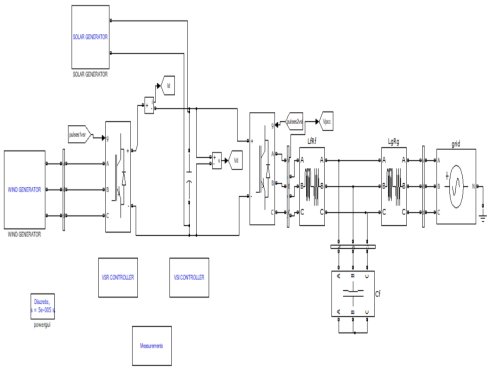

Fig. 3. Proposed wind-solar cogeneration system

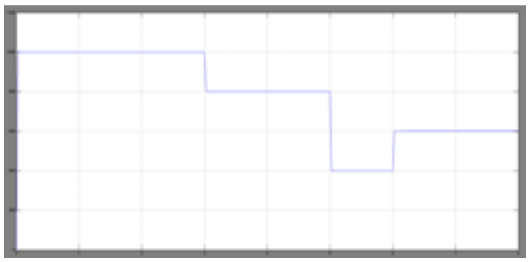

(a) solar irradiance

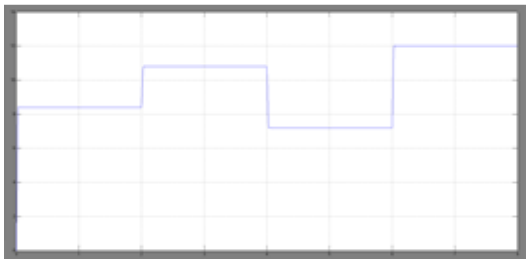

(b) wind speed

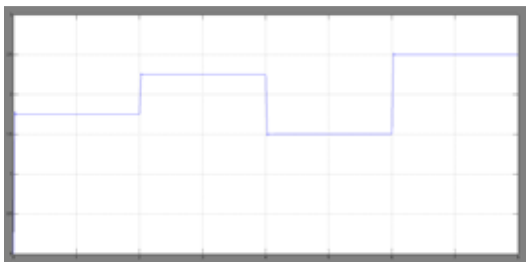

(c) PMSG speed

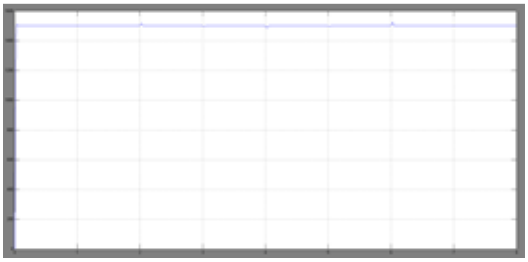

(d) DC link voltage

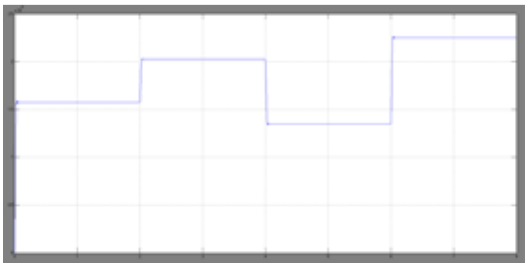

(e) Wind power

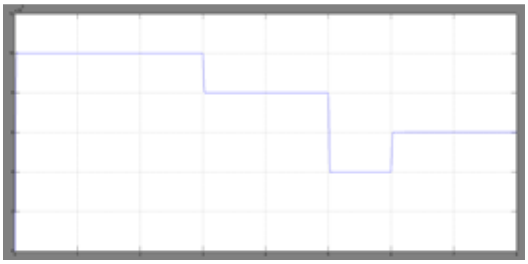

(f) PV Power

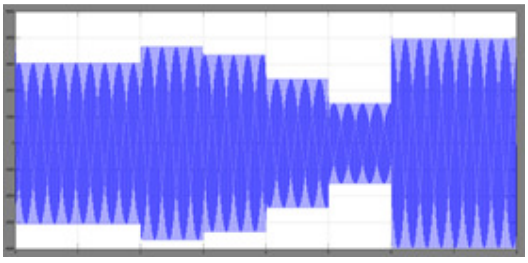

(g) Grid current

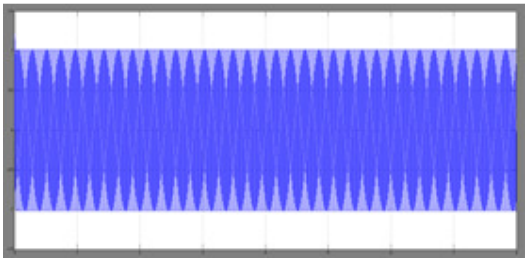

(h) PCC Voltage

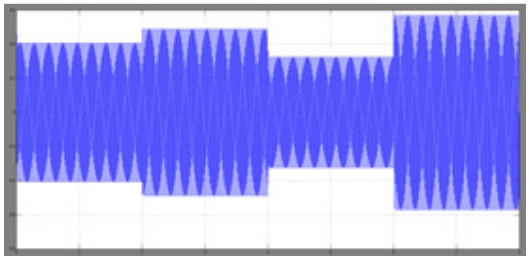

(i) VSR modulation

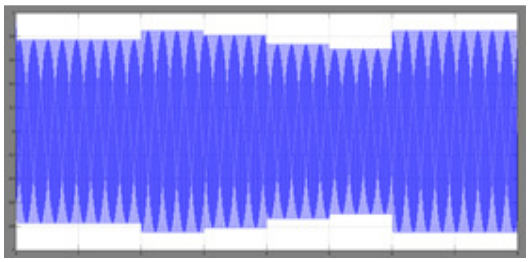

(j) VSI Modulation

Fig. 4 Performance of the wind and solar generators

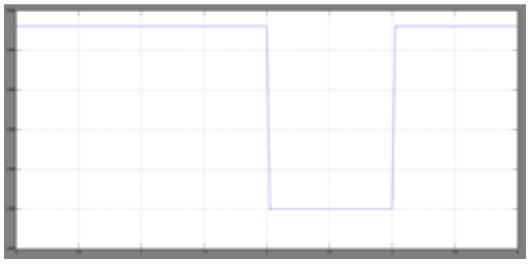

(a)

(b)

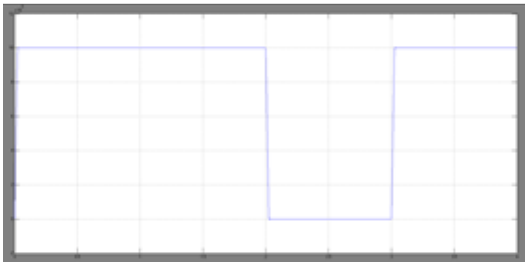

(c)

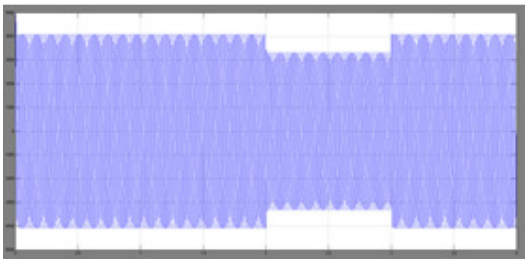

(d)

Fig.5 Performance of the wind generator only. (a) DC-link voltage. (b) Wind and (c)solar generated powers. (d) Injected ac current to the utility-grid.

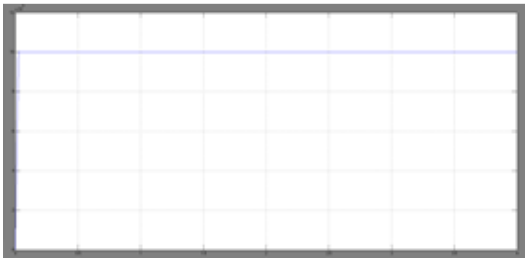

(c)

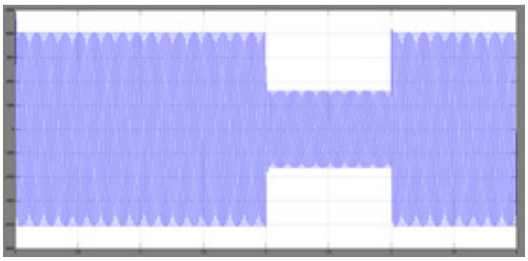

(d)

Fig. 6 Performance of the PV generator only. (a) PMSG speed. (b) Wind and (c)solar generated powers. (d) Injected ac current to the utility-grid.

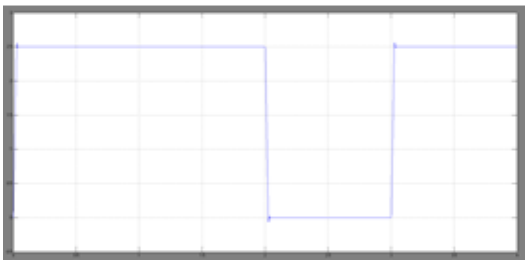

(a)

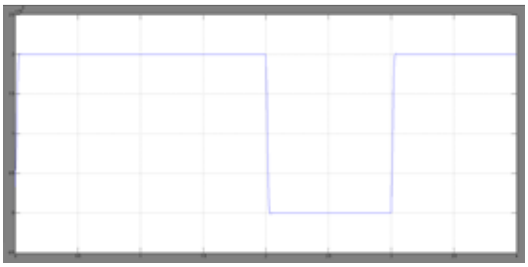

(b)

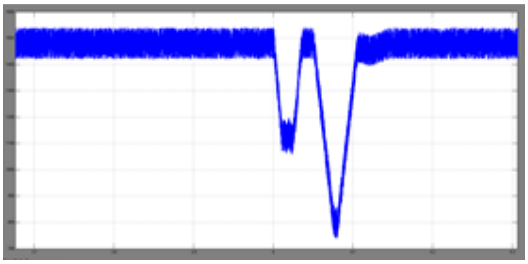

(a) DC link voltage

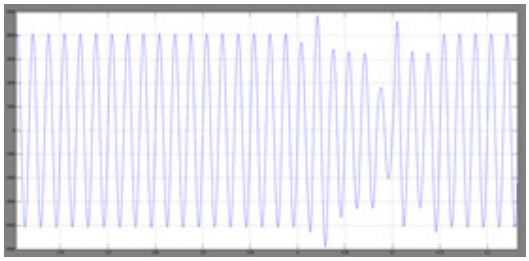

(b) Grid current

Fig.7 Response to a 3PG fault at t = 4.0 s for 4.0 cycles – 1.0 and 0.5 p.u. wind power generation with 1.0 p.u. solar power.

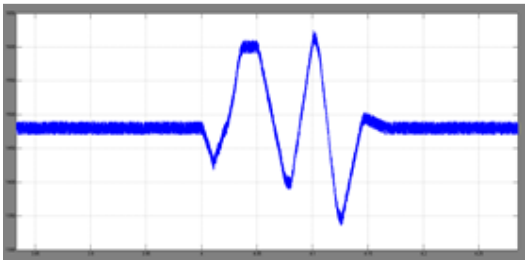

(a) DC link voltage

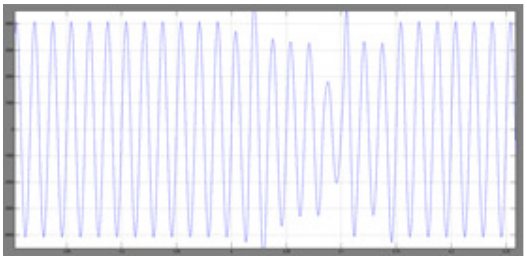

(b) Grid current

Fig.8 Response to a 3PG fault at t = 4.0 s for 4.0 cycles – 1.0 p.u. wind and solar power generation with implemented fault protection schemes.

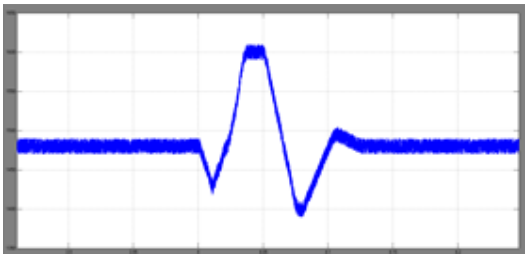

(a)DC link voltage

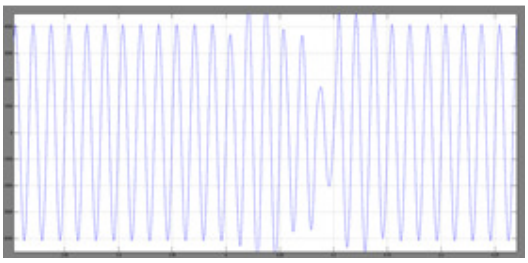

(b) Grid current

Fig.9 Response to a 1PG fault at t = 4.0 s for 4.0 cycles – 1.0 p.u. wind and solar power generation with and without the fault protection schemes

CONCLUSION

This paper has presented the combination of the wind and solar systems using vector-controlled grid-connected BtB VSCs. The VSR at the wind generator side is responsible for extracting the maximum wind power following the wind velocity variations. On the utility-grid side, the roles of the VSI are to extract the maximum PV power from the PV generator, achieve the balance between the input and output powers across the dc-link capacitor, and to maintain a unity PCC voltage under different modes of operation. A small-signal linearization analysis has been conducted where the entire state-space model is developed to investigate the system stability. The proposed system features the following advantages; 1) the increased reliability and efficiency due to the combined wind and solar generators. 2) the independent MPPT extraction as the VSR and VSI are solely responsible for extracting the wind and PV powers, respectively. 3) the regulation of the dc-link voltage under all operating conditions is maintained by the VSI and hence a better damped performance is yielded. 4) simple system structure and controller's design. 5) fault-ride through can be achieved using existing protection schemes. A well-damped performance and an efficient operation have been revealed from the time-domain simulations results under the MATLAB/Simulink environment under different operational scenarios

REFERENCES

[1] Renewable Energy Policy Network for the 21st Century, "Advancing the global renewable energy transition," REN21 Secretariat, Paris, France, 2017. [Online]. Available: http://www.ren21.net/wpcontent/uploads/2017/06/GSR2017_-Highlights.pdf

[2] F. Blaabjerg, Z. Chen, and S. B. Kjaer, "Power electronics as efficient interface in dispersed power generation systems," IEEE Trans. Power Electron., vol. 19, no. 5, pp. 1184–1194, Sep. 2004.

[3] J. Carrasco et al., "Power-electronic systems for the grid integration of renewable energy sources—a survey," IEEE Trans. Ind. Electron., vol. 53, no. 4, pp. 1002–1016, Jan. 2006.

[4] A. Yazdani and P. P. Dash, "A control methodology and characterization of dynamics for a photovoltaic (PV) system interfaced with a distribution network," IEEE Trans. Power Del., vol. 24, no. 3, pp. 1538–1551, Jul. 2009

[5] L. Nousiainen et al., "Photovoltaic generator as an input source for power electronic converters," IEEE

Trans. Power Electron., vol. 28, no. 6, pp. 3028–3038, Jun. 2013.

[6] N. Strachan and D. Jovcic, "Stability of a variable-speed permanent magnet wind generator with weak ac grids," IEEE Trans. Power Del., vol. 25, no. 4, pp. 2279–2788, Oct. 2010.

[7] P. Mitra, L. Zhang, and L. Harnefors, "Offshore wind integration to a weak grid by VSC-HVDC links using power-synchronization control— A case study," IEEE Trans. Power Del., vol. 29, no. 1, pp. 453–461, Feb. 2014.

[8] Y. Wang, J. Meng, X. Zhang, and L. Xu, "Control of PMSGbased wind turbines for system inertial response and power oscillation damping," IEEE Trans. Sustain. Energy, vol. 6, no. 2, pp. 565–574, Apr. 2015.

[9] F. Giraud, "Analysis of a utility-interactive wind-photovoltaic hybrid system with battery storage using neural network," Ph.D. dissertation, Dept. Electr. Eng., Univ. Massachusetts Lowell, Lowell, MA, USA , 1999.

[10] L. Xu, X. Ruan, C. Mao, B. Zhang, and Y. Luo, "An improved optimal sizing method for wind-solar-battery hybrid power system," IEEE Trans. Sustain. Energy, vol. 4, no. 3, pp. 774–785, Jul. 2013.

[11] S. Sarkar and V. Ajjarapu, "MW resource assessment model for a hybrid energy conversion system with wind and solar resources," IEEE Trans. Sustain. Energy, vol. 2, no. 4, pp. 383–391, Oct. 2011.

[12] Y.-M. Chen, Y.-C. Liu, S.-C. Hung, and C.-S. Cheng, "Multi-input inverter for grid-connected hybrid PV/wind power system," IEEE Trans. Power Electron., vol. 22, no. 3, pp. 1070–1077, May 2007.

[13] S. Bae and A. Kwasinski, "Dynamic modeling and operation strategy for microgrid with wind and photovoltaic resources," IEEE Trans. Smart Grid, vol. 3, no. 4, pp. 1867–1876, Dec. 2012.

[14] B. Mangu, S. Akshatha, D. Suryanarayana, and B. G. Fernandes, "Grid-connected PV-wind-battery-based multi-input transformer-coupled bidirectional dc-dc converter for household applications," IEEE Trans. Emerg. Sel. Topics Power Electron., vol. 4, no. 3, pp. 1086–1095, Sep. 2016.

[15] P. Shanthi, G. Uma, and M. S. Keerthana, "Effective power transfer scheme for a grid connected hybrid wind/photovoltaic system," IET Renew. Power Gener., vol. 11, no. 7, pp. 1005–1017, 2017.

[16] T. Hirose and H. Matsuo, "Standalone hybrid wind-solar power generation system applying dump power control without dump load," IEEE Trans. Ind. Electron., vol. 59, no. 2, pp. 988–997, Feb. 2012.

[17] K. Kant, C. Jain, and B. Singh, "A hybrid diesel-wind-PV based energy generation system with brushless generators," IEEE Trans. Ind. Inf., vol. 13, no. 4, pp. 1714–1722, Aug. 2017.

[18] U. Kalla, B. Singh, S. Murthy, C. Jain, and K. Kant, "Adaptive sliding mode control of standalone single-phase microgrid using hydro, wind and solar PV array based generation," IEEE Trans. Smart Grid., vol. 9, no. 6, pp. 6806–6814, Nov. 2018.

[19] A. Merabet, K. Ahmed, H. Ibrahim, R. Beguenane, and A. Ghias, "Energy management and control system for laboratory scale microgrid based wind-PV-battery," IEEE Trans. Sustain. Energy, vol. 8, no. 1, pp. 145– 154, Jan. 2017.

[20] M. Meiqin, S. Jianhui, L. Chang, Z. Guorong, and Z. Yuzhu, "Controller for 1 kW–5 kW wind-solar hybrid generation systems," in Proc. Can. Conf. Elect. Comput. Eng., Niagara Falls, ON, Canada, 2008, pp. 1175–1178.